

## Aerosol Optical Depth, Ozone and Water Vapor Measurements over Gadanki, A Tropical Station in Peninsular India

A. K. Srivastava<sup>1\*</sup>, P. C. S. Devara<sup>1\*</sup>, Y. Jaya Rao<sup>1</sup>, Y. Bhavanikumar<sup>2</sup>, D. N. Rao<sup>2</sup>

<sup>1</sup> *Indian Institute of Tropical Meteorology, Dr. Homi Bhabha Road, Pune, India*

<sup>2</sup> *National Atmospheric Research Laboratory, Gadanki, India*

---

### Abstract

This paper reports the results of a study related to the optical and physical characteristics of columnar aerosols and variation in total column ozone (TCO) and precipitable water content (PWC) over Gadanki (13.45°N, 79.18°E), a tropical station in peninsular India, for the first time, using MICROTOPS-II (Microprocessor-based Total Ozone Portable Spectrometer), comprising of both sun photometer and ozonometer. Results show wavelength dependence of AOD, having mean value of  $\sim 0.4$  ( $\pm 0.09$ ) at 500 nm optical channel. Daily mean aerosol size spectra shows, most of the time, power-law distribution. However, its diurnal variations show significant changes in aerosol size spectra modulated by a combination of both power-law and bi-modal distributions. To characterize AOD, the Ångström parameters (i.e.,  $\alpha$  and  $\beta$ ) were used. The day-to-day variations in TCO were found to be in fair agreement with that derived from TOMS satellite data for all the experimental days, having mean observed value of  $\sim 253$  ( $\pm 8$ ) DU over the station. Interestingly, an inverse relationship between TCO and AOD or PWC was observed over the station, on some times of the day, which could be attributed to the mixing of significant fraction of ozone with aerosol and water vapor-rich air mass. However, a significant positive correlation was observed between AOD and PWC.

**Keywords:** Aerosols; Aerosol optical depth; Ångström parameters; Total column ozone and precipitable water content.

---

### INTRODUCTION

Atmospheric aerosols, water vapor and ozone play key role in the study of the Earth's

climate system, because they interact with incoming as well as out-going solar radiation. Moreover, aerosols influence the solar radiation both directly and indirectly through their various sizes and thus their different optical and physical properties. When aerosols are sufficiently large in size, they scatter and absorb sun light, and when these particles are

---

\*Corresponding author(s). Tel: +91-11-28743976 and/or +91-20-25893600

E-mail address: atulmanish93@rediffmail.com

small, they act as cloud condensation nuclei and aid in the formation of clouds (Rosenfeld, 2006). Although the dynamics modifies the aerosol size spectrum during their residence time, the particle population highly depends on the strength of their source and sinks mechanisms. As a consequence, concentrations of ambient aerosol differ to a great extent between urban centers and remote areas, and between industrialized and rural regions (Rao *et al.*, 2001). On a global scale, the natural sources of aerosols are more important than the anthropogenic aerosols, but regionally anthropogenic aerosols are more important (Kaufman and Fraser, 1983; Ramanathan *et al.*, 2001).

Apart from atmospheric aerosols, ozone and water vapor content present in the atmosphere are also important atmospheric constituents that play key role in the radiation balance of the Earth-atmosphere system (Peixoto and Oort, 1983). Changes in tropospheric ozone are mainly associated with increase in the urban pollution and biomass burning. The column ozone concentration has been measured in the past by two well-known passive ground-based instruments, namely, Dobson and Brewer spectrophotometers (Komhyr *et al.*, 1989; Kerr and McElroy, 1995). But these instruments are very expensive, heavy and huge. There has been a need for less expansive, more portable and compact instruments that can measure ozone with reasonable accuracy over different environments. In the present study, a hand-held, advanced ozone monitor has been used to measure total column ozone (TCO) and its

variability over the experimental station.

Atmospheric aerosols and various gases interact in different ways with atmospheric water vapor and thus producing various effects. There have been a number of studies of the change of aerosol properties as a function of water vapor in terms of relative humidity (Hanel, 1972; Shettle and Fenn, 1979). Distribution of water content in the atmosphere is a good indicator of the dynamics of the circulation systems in the atmosphere (Raj *et al.*, 2004b). It is well known that the precipitable water content present in the atmosphere can vary at very short time scales (Bruegge *et al.*, 1992). Therefore, a continuous monitoring of precipitable water content with good temporal resolution is essential for understanding various dynamical processes occurring within the atmosphere. A sun photometer that has been used in the present study, works on the method of differential optical absorption and scattering (DOAS) that allows monitoring the precipitable water content in the atmosphere on a real-time scale with reasonable temporal resolution, which is otherwise difficult to make such measurements with other *in-situ* instruments.

## **EXPERIMENTAL SITE, MEASUREMENTS AND METHODOLOGY**

MICROTOPS-II (MICRO-processor based Total Ozone Portable Spectrometer), a compact, portable and multi-channel sun photometer, has been operated, for the first

time, at National Atmospheric Research Laboratory (NARL), Gadanki (13.45°N, 79.18°E and ~340 m above mean sea level), a tropical rural station, situated in the southern peninsular India, to study the characteristics of column aerosols, ozone and water vapor. The experimental site, Gadanki, is about 120 km inland from the east coast of India. The site is situated in a valley-like region, which is surrounded by hillocks of height ~200-700 m. Three-dimensional view of the main topography around Gadanki is shown in Fig. 1. The environment in the immediate vicinity of the experimental site is semi-urban, which is separated by a distance about 35 km having several small-scale industries nearby. Therefore, the possible aerosol type present over the station could be a mixture of water-soluble, dust-like and soot-type aerosols.

The observations were carried out using MICROTOPS-II. It consists of two sets of instruments: sun photometer that provides columnar AOD at five wavelengths of 380, 440, 500, 675, 870 nm and an ozonometer, which is capable of measuring the total column ozone (TCO) in Dobson Units (DU) using three UV channels (305.5, 312.5 and 320.0 nm) and the water vapor column (precipitable water content, PWC) in centimeters using two near-IR channels (940 and 1020 nm) as well as AOD at 1020 nm. Thus, the obtained AODs at total of six wavelengths from both the sets of MICROTOPS-II are utilized to retrieve the wavelength exponent, which is an index of aerosol size distribution.

Due to paucity of clear-sky conditions (when there are no visible clouds), the data obtained using both sets of instruments could be reported here only for the period from February 28-March 11, 2003, which were clear-sky days with maximum sampling duration on all days. Both the sets of instrument have the capability to make instantaneous measurements with high time resolution. In order to study the time history including short-scale variations in atmospheric constituents, instrument has been operated at 5-minute interval during sunrise and sunset period when the variation in solar zenith angle is faster, while the observations were carried out at 10-minute interval during intermediate period. Therefore, a total of about 60-70 data sets have been collected from sunrise to sunset period, on each experimental day.

Total optical depth in a vertical air column at wavelength  $\lambda$  was determined from the Beer-Lambert-Bouguer law, expressing total attenuation of direct solar beam through the atmosphere, in the form of

$$I(\lambda) = I_0(\lambda) \exp [-k \tau_t(\lambda)] \quad (1)$$

where  $I(\lambda)$  is the monochromatic solar irradiance reaching at the instrument detector,  $I_0(\lambda)$  is the irradiance incident at the top-of-atmosphere (TOA),  $k$  is the optical air mass, which is the mass of substances in a unit vertical cross-section and a function of solar zenith angle,  $\chi$  ( $k = \sec\chi$ ) and  $\tau_t(\lambda)$  is the total optical depth, which includes aerosol,  $\tau_a(\lambda)$ ;

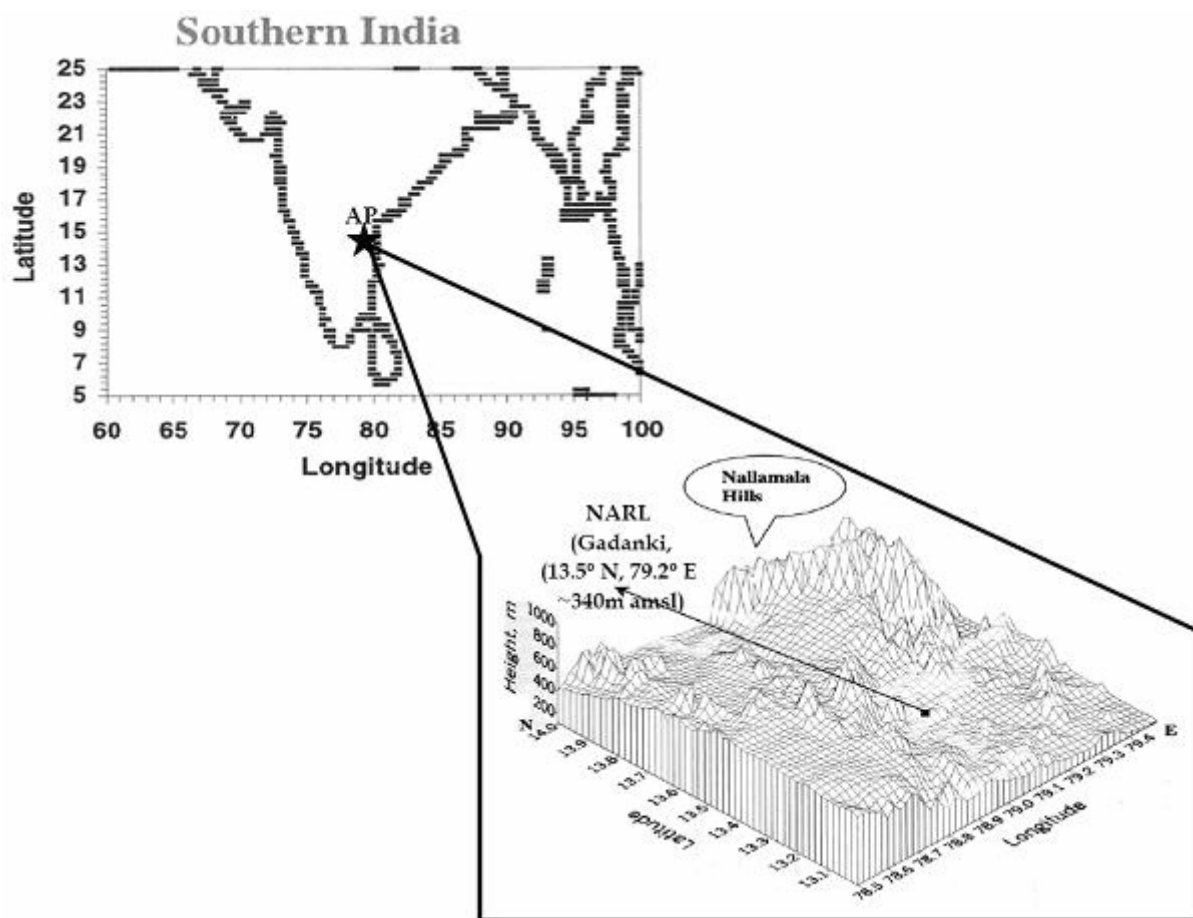


**Fig. 1.** Three-dimensional view of the topography around the experimental station, Gadanki.

molecular,  $\tau_m(\lambda)$  and gaseous,  $\tau_g(\lambda)$  optical depths. The slope of regression line provides the information about  $\tau_t(\lambda)$ . By subtracting  $\tau_m(\lambda)$  and  $\tau_g(\lambda)$  from  $\tau_t(\lambda)$ , we can obtain the value of  $\tau_a(\lambda)$ .

TCO, an equivalent to the thickness of pure ozone layer at standard temperature and pressure, is measured by recording the differential absorption of solar light intensity at wavelengths in the UV region (305.5 and 320.0 nm). The measurement at third wavelength (312.5 nm) is used to correct for particulate scattering and stray light (Devara *et al.*, 2001). On the other hand, PWC measurement is based on a pair of radiometric

measurements in near-IR band. The estimation of PWC was made by following the differential optical absorption method applied to the irradiance data archived at 940 and 1020 nm channels. The 940 nm channel is located in the strong water vapor absorption band whereas 1020 nm channel has negligible water vapor absorption but it is affected by aerosol scattering. Calculation of AOD at 1020 nm channel is based on the extra-terrestrial radiation at that wavelength, corrected for Sun-Earth distance, and the ground-level measurement of the radiation at 1020 nm (Morys *et al.*, 2001). Additional details of MICROTOS-II, used in the present study,

have been reported elsewhere (Devara *et al.*, 2001; Morys *et al.*, 2001; Ichoku *et al.*, 2002; Raj *et al.*, 2004a; 2004b).

Calibration of the radiometers is very essential for obtaining reliable results. Both the sets of MICROTOPS-II were freshly calibrated at Honolulu, Hawaii, a noise-free high-altitude site, by its manufacturer (M/S Solar Light Control, USA) before the measurements. Apart from this, continuous monitoring of MICROTOPS-II output at zero air mass (extra-terrestrial constant), which serves as calibration constant for each channel, and also inter-instrumental comparison of AOD with simultaneously operated spectroradiometer has been carried out periodically to ensure the stability and reliability of AOD, TCO and PWC. Besides calibration issues, error in the MICROTOPS-II measurements can also be caused by filter degradation, temperature effects and poor pointing at the sun. The pointing accuracy of the optical filters towards the sun, during each measurement, is very crucial for accurate measurement of atmospheric constituents (Morys *et al.*, 2001). In the present study, both the sets were operated using a common wooden platform with a precision elevation-azimuth assembly, so as to strictly maintain synchronization between the measured parameters in all respects, in addition to the stability of instruments and the pointing accuracy of each optical filter.

## **RESULTS AND DISCUSSION**

### ***Day-to-day Spectral Variation of AOD***

Knowledge on the spectral dependence of AOD is important for adequately modeling the effects of aerosols on the radiation budget of the Earth-atmosphere system or for accurately retrieving the aerosol optical parameters from satellite-remote sensors (Eck *et al.*, 1999). The wavelength dependence of AOD varies between different aerosol types because of their different physical and chemical characteristics. Fig. 2 shows daily variations in spectral distribution of AOD observed during February 28–March 11, 2003 in the wavelength range of 380–1020 nm. The vertical lines show standard deviation of AOD at each wavelength. Significant variations in wavelength dependence of AOD are evident from the figure. Although the sky was visibly clear on these days, the magnitude of AOD, particularly at wavelengths of 380, 440 and 500 nm, is found to be slightly higher on March 5, 7 and 8, 2003, respectively that reveals an indication of presence of optically thin sub-visible cloud/haze layers in the sensing region. An interesting feature was observed on March 11, 2003 when AOD values are found to be low as compared to the remaining days having less variability in all the optical channels. As noticed on the other days, AOD on March 11, 2003 was observed to be decreasing pattern with increasing wavelength except at 440 nm. The increase in AOD from 380 to 440 nm wavelength is due to having larger particles distribution.

### ***Day-to-day Variation of ASD***

The spectral distributions of AOD have been used to derive aerosol size distribution

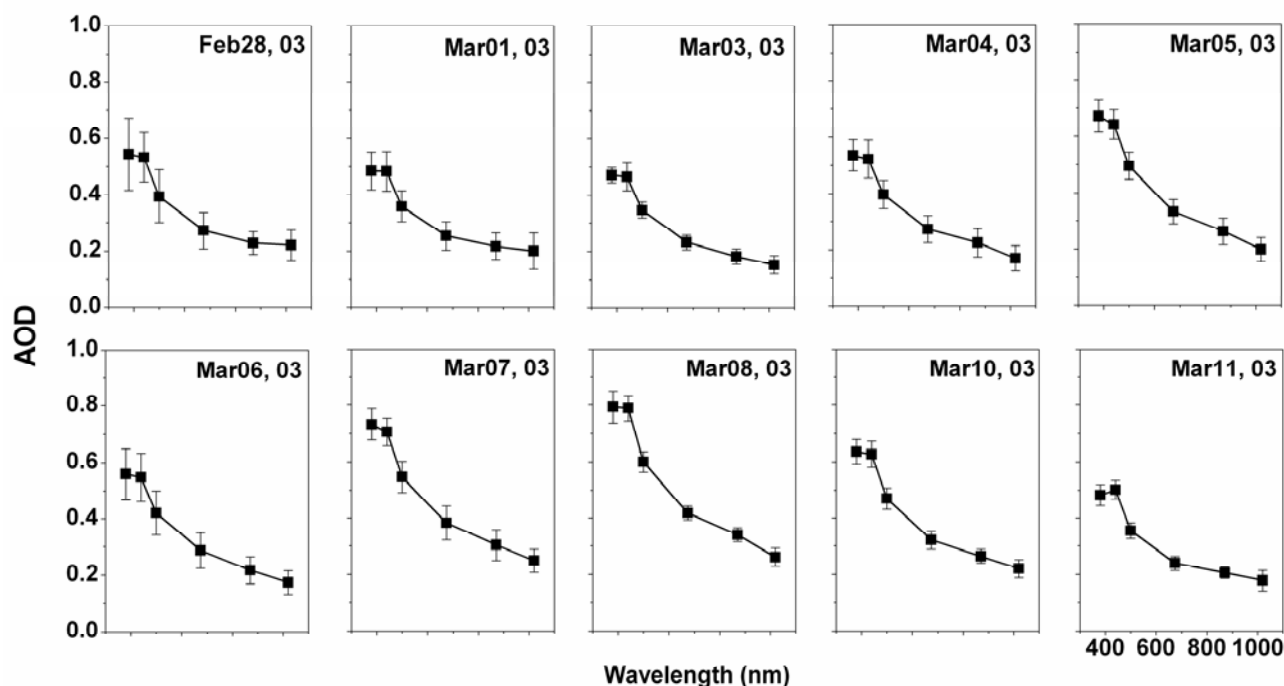


**Fig. 2.** Day-to-day spectral variations in AOD observed with MICROTOPs-II over Gadanki.

(ASD) by making use of the inversion technique suggested by King *et al.* (1978); King (1982). Fig. 3 shows day-to-day variations of ASD thus obtained. The size distribution results are presented in terms of  $dN_n/d\log r$ , which represent the number of particles per unit area per unit log radius interval in a vertical column through the atmosphere. Daily mean variation of ASD over the station exhibits power-law size distribution, except on March 11, 2003 when a bi-modal size distribution was observed, suggesting an enhanced loading of coarse-mode (natural origin) particles, which could be associated with an enhanced local activity such as wind-blown dust. The fine-mode (anthropogenic origin) aerosol particles were also observed on March 11, 2003, which was found to be lower as compared to that on other days.

As the experimental site is away from the anthropogenic activities, the occurrence of fine-mode aerosol particles, on most of the observation days, could be due to long-range transport of anthropogenically originated aerosols from their source regions. In order to study the above aspect, 5-days air mass back-trajectories obtained from the NOAA-ARL HYSPLIT model (<http://www.arl.noaa.gov/ready/hysplit4.html>) at three different height levels of 500, 1000 and 1500 m have been plotted in Figs. 4(a) and (b) for March 10 and 11, 2003, respectively. The three different levels are the representative heights of surface layer, within the boundary layer and in free troposphere, respectively. It is evident from both the figures that the air mass, at all the levels, originally coming from the Indo-Gangatic basin, which is one of the most polluted regions in the world (Dey and

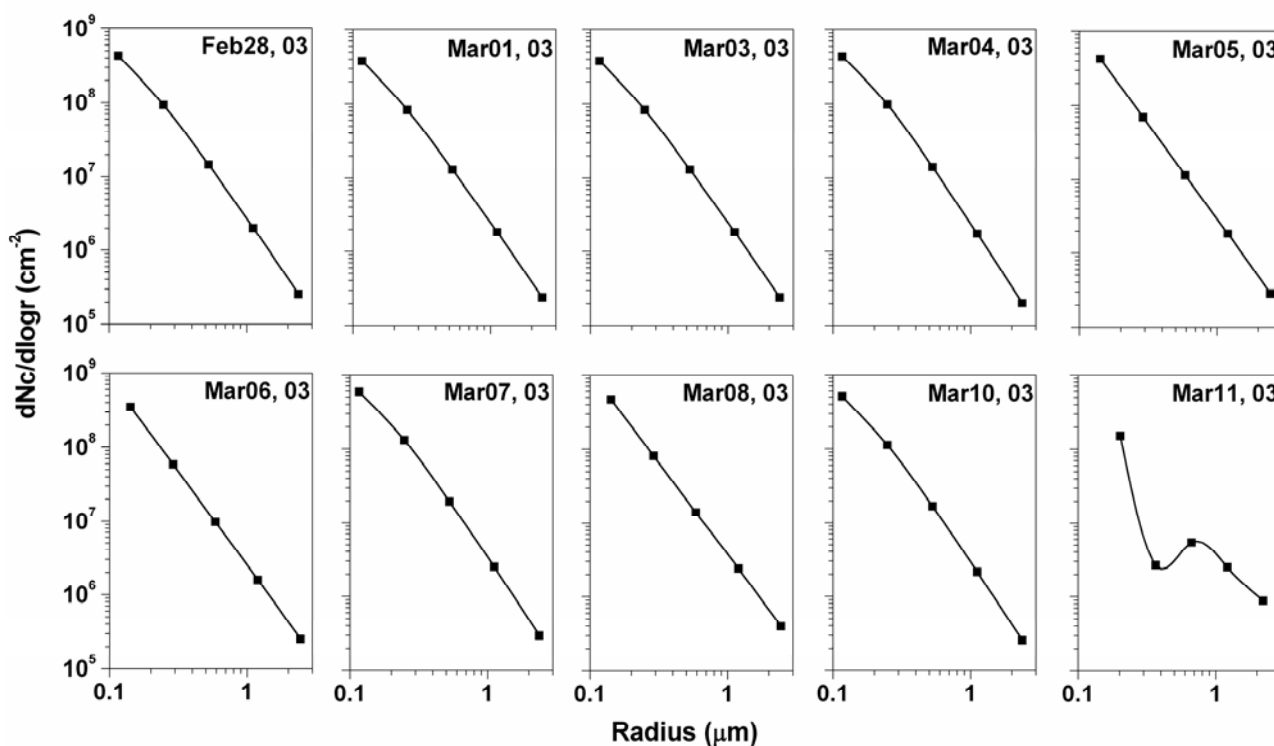


**Fig. 3.** Day-to-day variations in ASD derived from spectral variations in AOD.

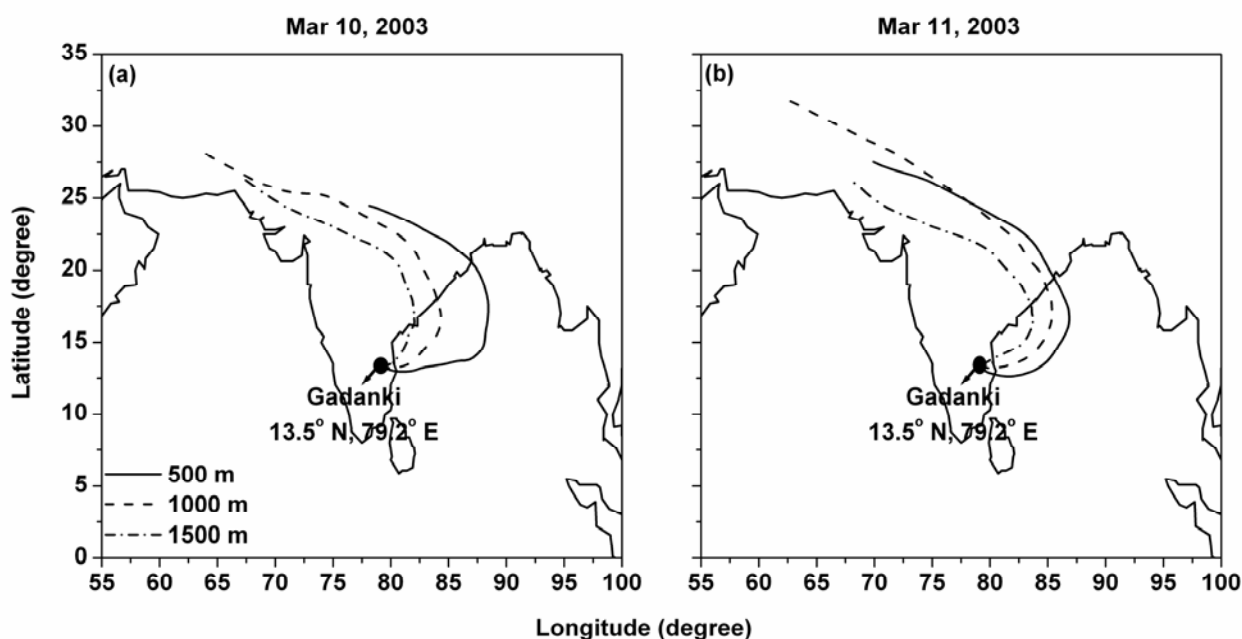


**Fig. 4.** 5-days air mass back-trajectories at three representative altitudes over Gadanki on (a) March 10, 2003 and (b) March 11, 2003.

Tripathi, 2007), and then reaches over the experimental site after passing through the

marine region of Bay-of-Bengal. Thus, the fine-mode anthropogenic aerosols bring

through air mass over the station get mixed with marine air, which dominate at the lower level (at 500 m) due to large marine regions covered by this level as compared to that at higher levels. As the station is surrounded by hillocks of height ~200-700 m, the influence of lower level air mass over the observing station, may not be much as compared to that at higher levels.

#### ***Day-to-day Variation of Mean AOD and Ångström Parameters***

Fig 5(a) shows daily variations in AOD at three characteristic wavelengths as 380, 500 and 1020 nm, representing the fine, accumulation and coarse modes of aerosol particles, respectively. Large AOD values having large variability on all the days have been observed at lower wavelengths, which decrease with increasing wavelength. Peak AOD at all the three wavelengths was observed on some of the days, indicating the presence of haze/optically thin sub-visible clouds as discussed previously in Fig. 2.

The wavelength dependence of AOD is usually represented by the Ångström coefficients (Ångström, 1961) such as Ångström exponent ( $\alpha$ ) and turbidity coefficient ( $\beta$ ), which indicates size and concentration of aerosol particles, respectively. Daily variation of  $\alpha$  and  $\beta$ , ranging from ~1.0-1.3 and ~0.15-0.27, respectively is shown in Fig. 5(b). An inverse relationship between these two parameters was observed on most of the experimental days, i.e. the low  $\alpha$  values are associated with the high  $\beta$  values and vice-versa, which agrees with earlier observations

by Dani *et al.* (2003); Satheesh *et al.* (2006). The relatively smaller values of  $\alpha$  indicate the presence of coarse-mode particles; however, larger values indicate the presence of fine-mode particles over the station.

#### ***Temporal Variation of AOD, ASD and Ångström Parameters***

The capability of MICROTOSPS-II to make high resolution measurements has been used to study the temporal variations in AOD, ASD and Ångström parameters (derived from spectral AOD). Such a study is very significant to understand the variability of aerosol loading having different sizes. Fig. 6 depicts the temporal variation of AOD for optical channels 380, 500 and 1020 nm on a typical clear-sky days on March 11, 2003. It is evident that the AOD values are almost constant at all the wavelengths till the noon time 12:30 hrs where a sharp enhancement in AOD was observed at higher wavelength (1020 nm), which is found to decrease afterwards. The peak during the mid-day hours could be attributed to the local convective activity leading to change in aerosol particle number distributions. On the other hand, a slight enhancement in AOD has been observed on other two lower wavelengths in the afternoon hours. Moreover, sharp enhancement in AOD was observed during 15:30 hrs at smaller wavelengths (380 and 500 nm), which results in horizontal advection of pollution leading to higher aerosol column content. These results are in the general agreement with those reported earlier by different investigators (Shaw, 1979;



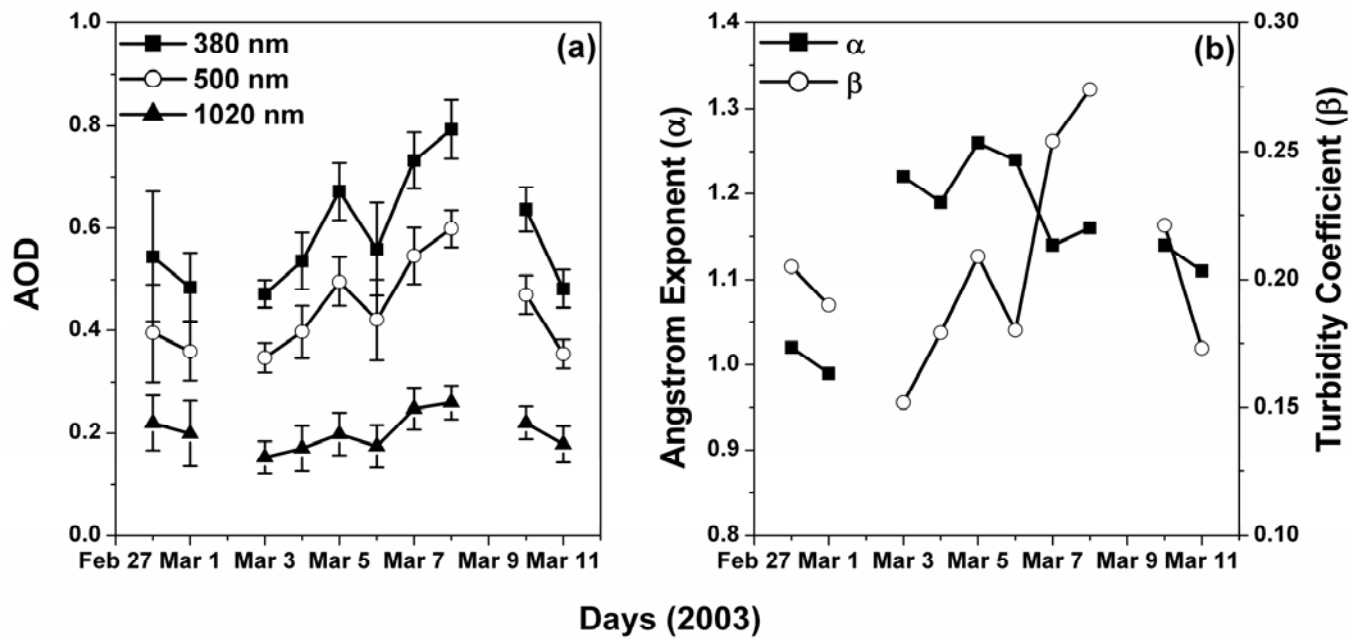


**Fig. 5.** Day-to-day variations in (a) AOD at three characteristic wavelengths (380, 500 and 1020 nm), representing the fine, accumulation and coarse modes of aerosol particles, respectively and (b) Ångström parameters.

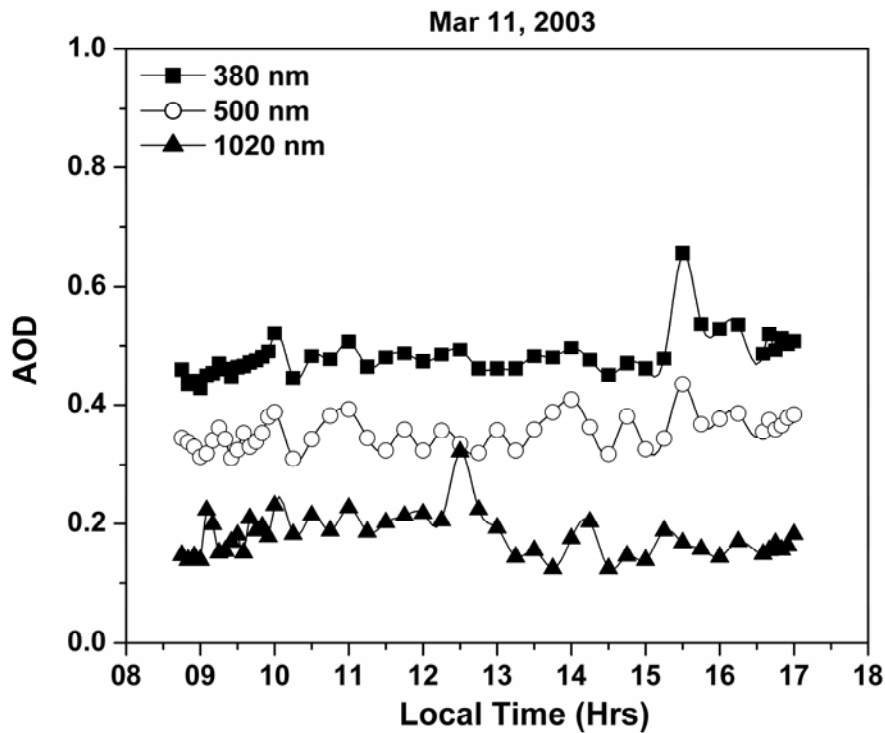


**Fig. 6.** Day-time diurnal variations in AOD at three representative wavelengths (380, 500 and 1020 nm) over Gadanki on March 11, 2003.

Pinker *et al.*, 1994; Devara *et al.*, 1996; Latha and Badarinath, 2005; Ganesh *et al.*, 2008).

As explained above, the observed temporal variation of AOD for different optical channels has been utilized to study the temporal variation of ASD. Hourly mean values of AOD for different optical channels have been utilized for this purpose. Fig. 7 displays hour-to-hour variations in ASD observed over the station on March 11, 2003. Significant variations in ASD with time are clearly evident from this figure. The ASDs show bi-modal distribution almost up to afternoon hours indicating an enhanced loading of coarse-mode aerosol particles along with fine-mode particles over the station, as already depicted in the temporal AOD variation at higher wavelength in Fig. 6. It is interesting to note here that the bi-modal nature of aerosol size distribution slowly turns into the power-law size distribution by the evening hours indicating the abundance of fine-mode particles.

Fig. 8 compares the temporal variations of  $\alpha$  and  $\beta$  observed on same day as discussed before. It reveals variations in different sizes of particles with variable aerosol loading, which are showing inverse relationship, as already discussed. Significant changes in both the Ångström parameters have been observed in the afternoon hours (12:30 hrs) when a sharp increase in  $\alpha$  values with significant decrease in  $\beta$  values were observed, indicating significant abundance of fine-mode particles in the afternoon hours till evening as compared to the coarse-mode. However, opposite feature was observed in the forenoon

hours when the significant abundance of coarse-mode particles was observed. The dominance of coarse-mode particles in the forenoon hours and fine-mode particles in the afternoon hours has been clearly seen and discussed in the hourly variations in ASD.

### ***Columnar Ozone and Precipitable Water Content Measurements***

In addition to the aerosol measurements, ozonometer version of MICROTOS-II provides TCO and PWC by making use of differential absorption of irradiance at 305, 312 and 320 nm for ozone and 940 and 1020 nm for retrieving the precipitable water content. High resolution measurements of columnar ozone and water vapor from MICROTOS-II have been used to examine the temporal variation of these parameters. Fig. 9 portrays temporal variations of ozone (with solid rectangles) and PWC (with open circles) observed over the station during February 28–March 11, 2003. Day-to-day variations in ozone concentration and PWC can be seen from this figure with significant fluctuations, which were observed to be large on February 28 and March 01, 2003 throughout the measurements and embedded with significant short-term fluctuations on the other days of observations. Two significant peaks in ozone concentrations were observed in the morning and evening hours of most of the days; however a dip in ozone values was observed in the noon hours. During daytime, photochemical reactions take place in the presence of sunlight and  $\text{N}_2\text{O}_5$  that formed due to oxidation of  $\text{NO}_2$  during night,

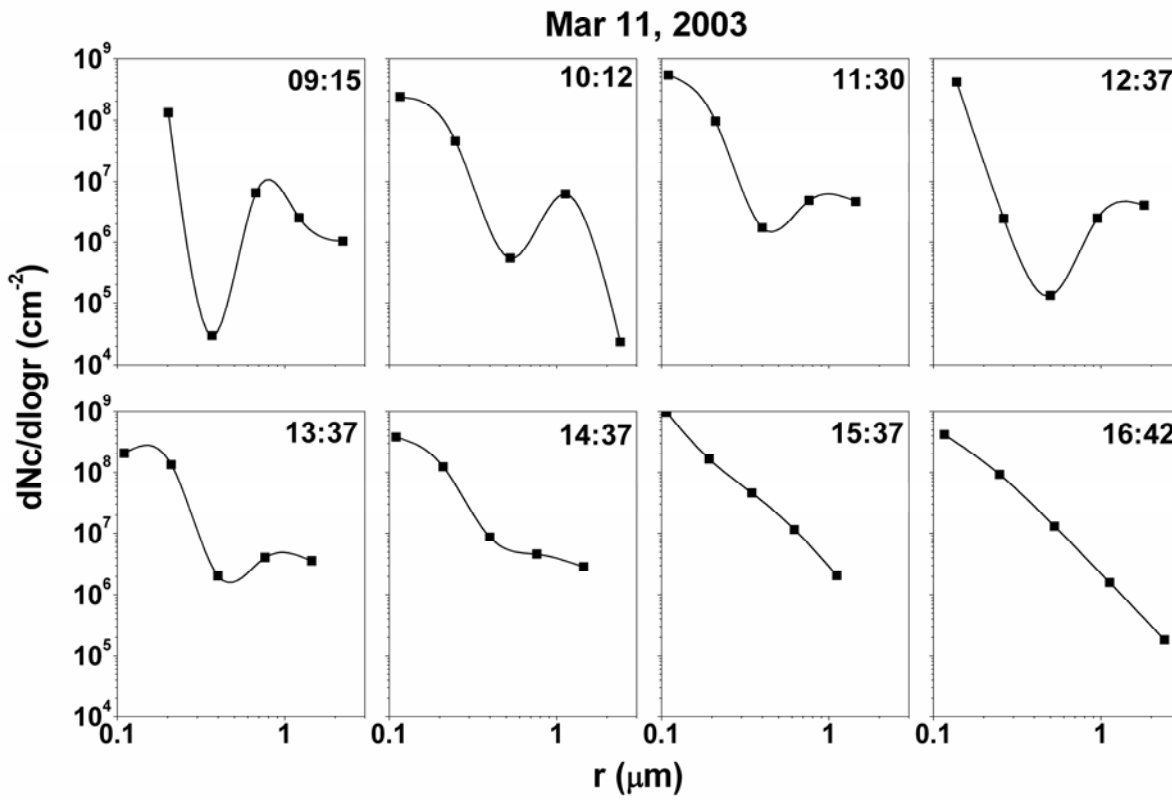


Fig. 7. Hourly variations in ASD over Gadanki on March 11, 2003.

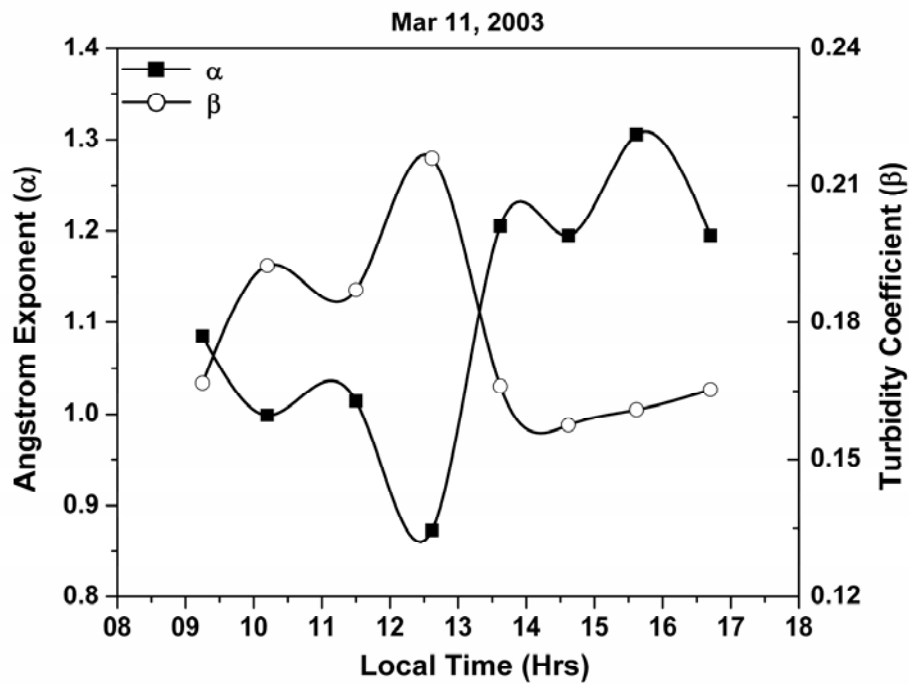
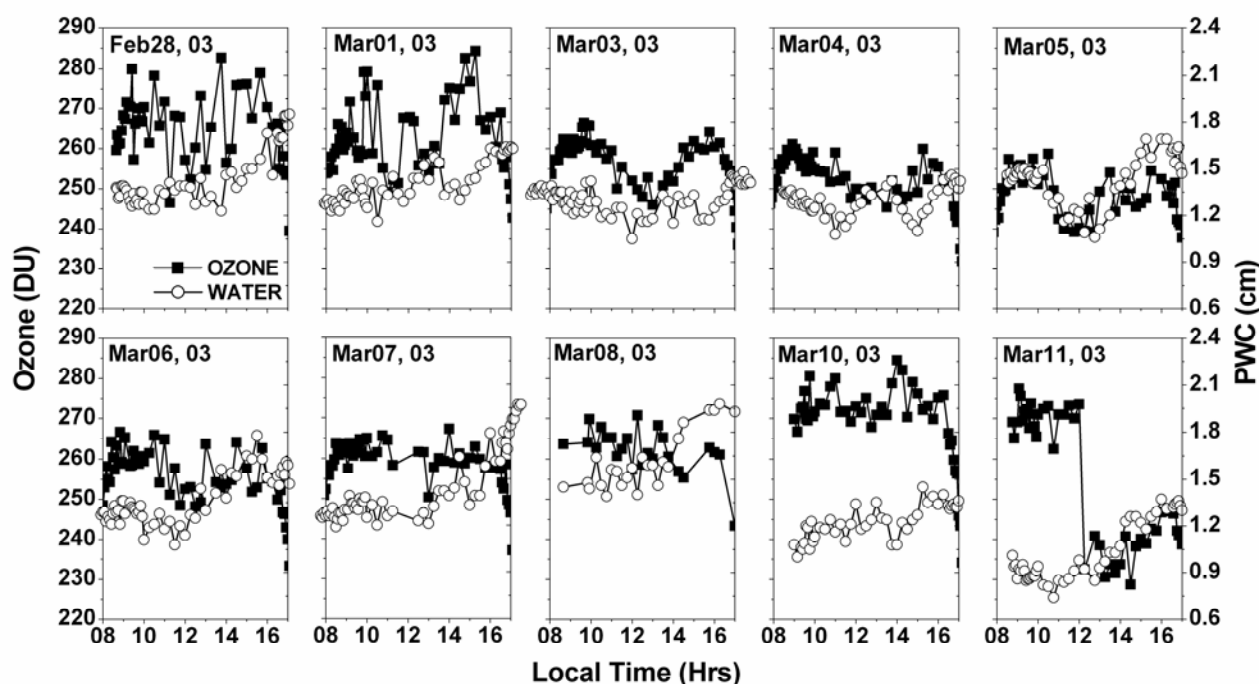


Fig. 8. Temporal variations in Ångström parameters over Gadanki on March 11, 2003.



**Fig. 9.** Daily temporal variations in TCO (with solid rectangles) and PWC (with open circles) observed by MICROTOPS-II over Gadanki.

get photolyzed to reproduce  $\text{NO}_2$  (Kostadinov *et al.*, 1999). Various nitrogen oxides like  $\text{NO}$ ,  $\text{NO}_2$ ,  $\text{NO}_3$  etc. thus formed due to reaction with ozone affects its abundance. Thus, the depletion in TCO observed around noon hours, in the present study, is considered to be due to (i) scavenging by nitrogen oxides and (ii) minimum optical path-length. On the other hand, the variations in PWC show opposite trend over the station during noon hours when an enhancement in PWC was observed other than during the morning and evening hours, respectively. The results are slightly different as observed by Raj *et al.* (2004a); (2004b) over an urban station Pune.

The mean column ozone over the station was observed within the range from 243-264 DU during the study period, which is lower as reported by Raj *et al.* (2004a); Kalapureddy *et*

*al.* (2008) over different environments. On the other hand, the temporal variation of PWC over the station shows maximum frequency of occurrence of mean PWC ranging between 1.0 and 1.6 cm, which is higher as reported by Raj *et al.* (2004b) over an urban station, Pune. An interesting feature of sudden fall in ozone concentration ( $\sim 40$  DU) was also noticed on March 11, 2003 at about noon hours, which is continued till the end of observations as already seen in the corresponding aerosol measurements. On the other hand, the PWC values were observed to be increased till the end of measurements.

In order to investigate the compatibility between the TCO variations obtained from ground-based and satellite techniques, MICROTOPS-II determined TCO values are compared with those derived from Earth

Probe-Total Ozone Mapping Spectrometer (TOMS) satellite of NASA over the station for all the measurement periods, as shown in Fig. 10. The overpass time of TOMS satellite from the experimental station is around 12:00 noon. Thus, the comparison of TCO measured by MICROTOSPS-II was made within 30 minutes of the satellite derived TCO for its appropriateness (Fig. 10). The ground-based TCO values overestimate, by and large, the TOMS derived ozone but a fairly good agreement between these two techniques was noticed with an average difference  $\sim 9$  DU. The vertical lines at each data point in the figure indicate the standard deviation of ozone measured by MICROTOSPS-II. Raj *et al.* (2004a) have used similar instrument to measure TCO over a tropical urban station, Pune and studied its variability using five-year data. They have also found a good correspondence in TCO obtained from ground-based and TOMS satellite measurements over Pune. Recently, Kalapureddy *et al.* (2008) have made ship-based sun photometric measurements of TCO over Oceanic regions around the Indian sub-continent and compared with the TOMS derived ozone. They have found an overestimation of ship-based TCO values to the TOMS derived ozone values with an average difference  $\sim 23$  DU having in-phase day-to-day variations. The difference in the magnitude of ozone derived from two different techniques could be due to the fact that the ozonometer observations are made from a platform close to the Earth's surface and pointing skywards and the daily ozone

values are average of about 60-70 measurements collected from morning to evening; however, the satellite is downward pointed and the ozone values are instantaneous during the passage of the satellite over the particular location (Kalapureddy *et al.*, 2008).

#### ***Association between Columnar AOD, PWC and TCO***

Fig. 11 shows daily variations in columnar AOD at 500 nm (with solid circles), PWC (with open circles) and TCO (with open stars) over the experimental station during February 28–March 11, 2003. The mean column values of AOD, PWC and ozone were observed about  $0.4 (\pm 0.09)$ ,  $1.4 (\pm 0.2)$  cm and  $253 (\pm 8)$  DU, respectively over Gadanki. A significant positive correlation between AOD and PWC was observed, suggesting the growth of aerosol particles, which are hygroscopic in nature, on the occasions associated with higher PWC values. On the other hand, an opposite nature of relationship was observed, on some times of the day in TCO with those in PWC or AOD. The results may be attributed to the mixing of significant fraction of observed ozone with aerosol and water vapor-rich air mass that results an influence of aqueous-phase and surface-ozone or heterogeneous chemistry, key responsible for the ozone losses (Lelieveld and Crutzen, 1990; Bonasoni *et al.*, 2004). Dentener *et al.* (1996) have reported from their modeling studies that the ozone destruction on mineral aerosol surfaces could lead to 10% reduction of ozone concentration. In fact, the large surface area of solid particles may play a significant role as a

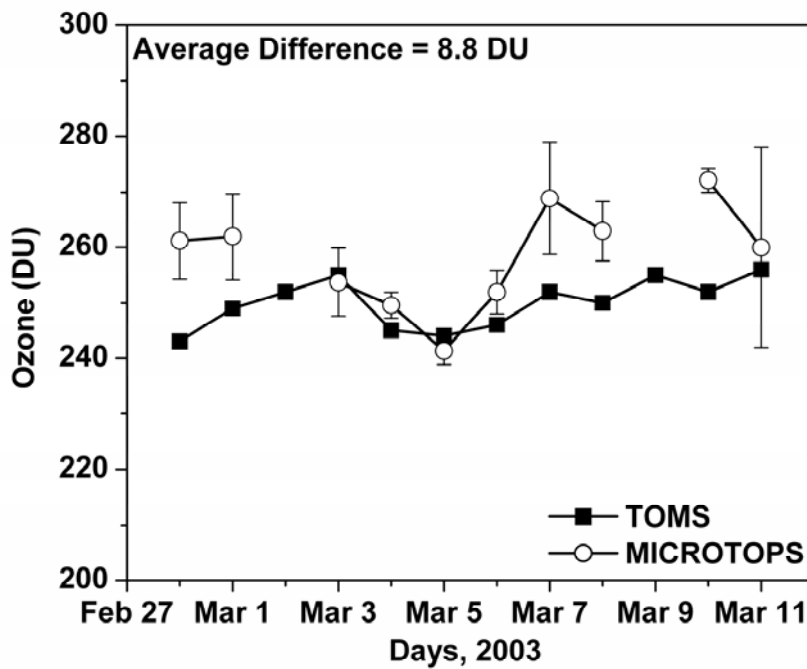


Fig. 10. Comparison of TCO obtained by MICROTOPS-II and TOMS satellite.

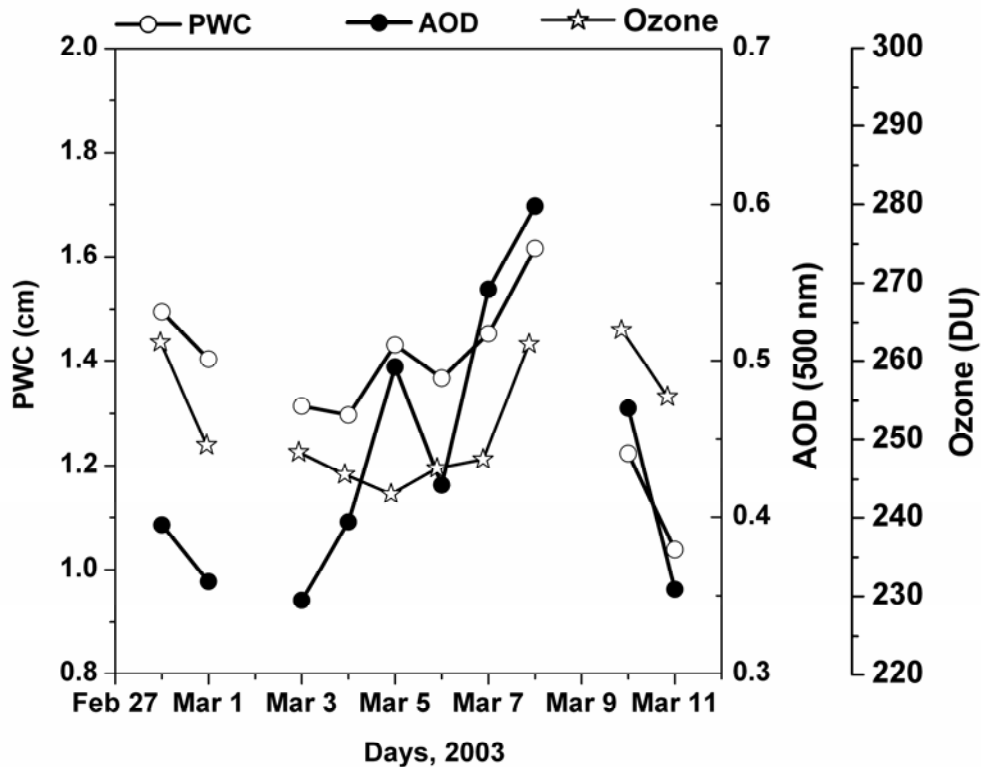


Fig. 11. Daily variations in columnar AOD at 500 nm (with solid circles), PWC (with open circles) and TCO (with open stars) over Gadanki.

reactive surface on which heterogeneous chemistry can take place (Zhang *et al.*, 1994).

## CONCLUSIONS

High resolution measurements of optical and microphysical properties of atmospheric aerosols and the variations of TCO and PWC have been carried out using MICROTUPS-II (sun photometer and ozonometer) at a tropical rural station, Gadanki in southern peninsular India. Results show significant spectral as well as day-to-day variations of AOD for different optical channels over the station. Mean aerosol size distributions show power-law distribution on most of the observation days; however, its diurnal variations show significant changes in aerosol size spectra modulated by a combination of both power-law and bi-modal distributions. The Ångström parameters, indicators of aerosol size distribution, show an inverse relationship. A good comparison was noticed between the ozonometer and TOMS observations of TCO over the station. Day-to-day variations in columnar AOD, PWC and ozone show significant positive correlation between AOD and PWC; however, by and large opposite trends were observed in TCO with AOD or PWC, on some times of the day, which is consistent with such measurements reported earlier from Pune, an urban station in India.

## ACKNOWLEDGEMENTS

The research work presented in this paper was supported by the Indian Space Research

Organization (ISRO), Department of Space, Government of India under RESPOND program. One of the authors (AKS) wishes to thank the Directors of IITM, Pune and ARIES, Nainital for their keen interest and encouragement. The back-trajectories used in this study were obtained from NOAA-ARL website. Authors are grateful to the two anonymous reviewers for their constructive and valuable comments/suggestions, which helped to improve the clarity of scientific content of the paper.

## REFERENCES

- Ångström, A. (1961). Techniques of Determining the Turbidity of the Atmosphere. *Tellu.* 8: 214-223.
- Bonasoni, P., Cristofanelli, P., Calzolari, F., Bonafe, U., Evangelista, F., Stohl, A., Zauli, S., Dingenen, R., Colombo, T. and Balkanski, Y. (2004). Aerosol-Ozone Correlations During Dust Transport Episodes. *Atmos. Chem. Phys.* 4: 1201-1215.
- Bruegge, C.J., Conel, J.E., Green, R.O., Margolis, J.S., Holm, R.G. and Toon, G. (1992). Water Vapor Column Abundance Retrievals During FIFE. *J. Geophys. Res.* 97: 18759-18768.
- Dani, K.K., Mahes Kumar, R.S. and Devara, P.C.S. (2003). Study of Total Column Atmospheric Aerosol Optical Depth, Ozone and Precipitable Water Content Over Bay of Bengal During BOBMEX-99. *Proc. Indian Acad. Sci. (Earth. Planet. Sci.)* 112: 205-221.

- Dentener, F.J., Carmichael, G.R., Zhang, Y., Lelieveld, J. and Crutzen, P.J. (1996). The Role of Mineral Aerosols as a Reactive Surface in the Global Troposphere. *J. Geophys. Res.* 101: 22869-22889.
- Devara, P.C.S., Maheshkumar, R.S., Raj, P.E., Dani, K.K. and Sonbawne, S.M. (2001). Some Features of Columnar Aerosol Optical Depth, Ozone and Precipitable Water Content Observed Over Land During the INDOEX-IFP 99. *Meteorologische Zeitschrift*. 10: 901-908.
- Devara, P.C.S., Pandithurai, G., Raj, P.E. and Sharma, S. (1996). Investigations of Aerosol Optical Depth Variations Using Spectroradiometer at an Urban Station, Pune, India. *J. Aerosol Sci.* 27: 621-632.
- Dey, S. and Tripathi, S.N. (2007). Estimation of Aerosol Optical Properties and Radiative Effects in the Ganga Basin, Northern India, During the Wintertime. *J. Geophys. Res.* 112: D03203, doi: 10.1029/2006JD007267.
- Eck, T.F., Holben, B.N., Reid, J.S., Dubovic, O., Smirnov, A., O'Neil, N.T., Slutsker, I. and Kinne, S. (1999). Wavelength Dependence of the Optical Depth of Biomass Burning, Urban, and Desert Dust Aerosols. *J. Geophys. Res.* 104: 31333-31349.
- Ganesh, K.E., Umesh, T.K. and Narasimhamurthy, B. (2008). Site specific aerosols optical thickness characteristics over Mysore. *Aerosol Air Qual. Res.* 8: 295-307.
- Hanel, G. (1972). Computation of the Extinction of Visible Radiation by Atmospheric Aerosol Particles as a Function of the Relative Humidity, Based Upon Measured Properties. *J. Aerosol Sci.* 3: 377-386.
- Ichoku, C., Levy, R., Kaufman, Y.J., Remer, L.A., Li, R.-R., Martins, V.J., Holben, B.N., Abuhassan, N., Slutsker, I., Eck, T.F. and Pietras, C. (2002). Analysis of the Performance Characteristics of the Five-Channel Microtops-II Sun Photometer for Measuring Aerosol Optical Thickness and Precipitable Water Vapor. *J. Geophys. Res.* 107 (D13): 4179, doi: 10.1029/2001JD001302.
- Kalapureddy, M.C.R., Raj, P.E. and Devara, P. C.S. (2008). Total Column Ozone Variations over Oceanic Region Around Indian Sub-Continent During Pre-Monsoon of 2006. *Atmos. Chem. Phys. Discuss.* 8: 3143-3162.
- Kaufman, Y.J. and Fraser, R.S. (1983). Light Extinction by Aerosols During Summer Air Pollution. *J. Clim. Appl. Meteorol.* 22: 1694-1725.
- Kerr, J.B. and McElroy, C.T. (1995). Total Ozone Measurements Made With the Brewer Ozone Spectrophotometer During STOIC 1989. *J. Geophys. Res.* 100: 9225-9230.
- King, M.D. (1982). Sensitivity of Constrained Linear Inversion to the Selection of the Lagrange Multiplier. *J. Atmos. Sci.* 39: 1356-1369.
- King, M.D., Byrne, D.M., Herman, B.M. and Reagan, J.A. (1978). Aerosol Size Distributions Obtained by Inversion of Spectral Optical Depth Measurements. *J. Atmos. Sci.* 35: 2153-2167.



- Komhyr, W.D., Grass, R.D. and Leonard, R.K. (1989). Dobson spectrophotometer 83: A Standard for Total Ozone Measurements, 1962-1987. *J. Geophys. Res.* 94 (D7): 9847-9861, 10.1029/89JD00473.
- Kostadinov, I., Giovanelli, G., Ravegnani, F., Bortoli, D. and Petritili, A. (1999). Depolarization Ratio of the Zenith Scattered Radiation and Measured NO<sub>2</sub> Slant Columns. *Proc. Soc. of Photo-Opt. Instrum. Eng. (SPIE)*. 3754: 402-410.
- Latha, K.M. and Badrinath, K.V.S. (2005). Factors Influencing Aerosol Characteristics Over Urban Environment. *Environ. Monit. and Assess.* 104: 269 – 280.
- Lelieveld, J. and Crutzen, P.J. (1990). Influence of Cloud Photochemical Processes on Tropospheric Ozone. *Nature*. 343: 227-233
- Morys, M., Mims III, F.M., Hagerup, S., Anderson, S. E., Baker, A., Kia, J. and Walkup, T. (2001). Design, Calibration, and Performance of MICROTOPS II hand-held Ozone Monitor and Sun Photometer. *J. Geophys. Res.* 106: 14573–14582.
- Peixoto, J.P. and Oort, A.H. (1983). The Atmospheric Branch of the Hydrological Cycle and Climate. *Variations in the Global Water Budget*, A. Street-Perrott, M. Beran, and R. Ratcliff, Eds., D. Reidel, p. 5–65.
- Pinker, R.T., Idemudia, G. and Aro, T.O. (1994). Characteristic Aerosol Optical Depths During the Harmattan Season in Sub-Saharan Africa. *Geophys. Res. Lett.* 21: 685.
- Raj, P.E., Devara, P.C.S., Pandithurai, G., Maheshkumar, R.S., Dani, K.K., Saha, S.K. and Sonbawne, S.M. (2004a). Variability in Sun Photometer-Derived Total Ozone Over a Tropical Urban Station. *J. Geophys. Res.* 109: D08309, doi: 10.1029/2003JD004195.
- Raj, P.E., Devara, P.C.S., Maheshkumar, R.S., Pandithurai, G., Dani, K.K., Saha, S.K., Sonbawne, S.M. and Tiwari, Y.K. (2004b). Results of Sun Photometer-Derived Precipitable Water Content Over a Tropical Indian station. *J. Appl. Meteorolo.*, 43: 1452-1459.
- Ramanathan, V., Crutzen, P.J. and Lelieveld, J. (2001). Indian Ocean Experiment: An Integrated Analysis of the Climate Forcing and Effects of the Great Indo-Asian Haze. *J. Geophys. Res.* 106: 28371-28398.
- Rao, P.S.P. , Momin, G.A., Safai, P.D., Ali, K., Naik, M.S. and Pillai, A.G. (2001). Aerosol and Ttrace Gas Studies at Pune During INDOEX IFP-99. *Curr. Sci.* 80: 105-109.
- Rosenfeld, D. (2006). Aerosols, Clouds and Climate. *Science* 312: 1323-1324.
- Satheesh, S.K., Moorthy, K.K., Kaufman, Y.J. and Takemura, T. (2006). Aerosol Optical Depth, Physical Properties and Radiative Forcing Over the Arabian Sea. *Meteorol. Atmos. Phys.* 91: 45-62.
- Shaw, G.F. (1979). Aerosols at Mauna Loa: Optical Properties. *J. Atmos. Sci.* 36: 862–872.
- Shettle, E.P., and Fenn, R.W. (1979). Models for the Aerosols of the Lower Atmosphere and the Effects of Humidity Variations on Their Optical Properties. *Air Force Geophysical Lab. Tech. Rep.* AFGL-TR-79-0214, p. 94.

Zhang, Y., Sunwoo, Y., Kotamarthi, V. and Carmichael, G.R. (1994). Photochemical Oxidant Pro-Processes in the Presence of Dust: An Evaluation of the Impact of Dust

on Particulate Nitrate and Processes Ozone Formation. *J. Appl. Met.* 33: 813-824.

*Received for review, May 21, 2008*

*Accepted, September 18, 2008*